Journal of Applied Electrochemistry **33**: 1–8, 2003.

Preparation of methanol oxidation electrocatalysts: ruthenium deposition on carbon-supported platinum nanoparticles

F. MAILLARD, F. GLOAGUEN and J-M. LEGER*
Equipe Electrocatalyse, LACCO, UMR 6503 CNRS - Université de Poitiers, 40, avenue du Recteur Pineau, 86022 Poitiers cedex, France
*(*author for correspondence, fax: +33 549453580, e-mail: jean.michel.leger@univ-poitiers.fr)*

Received 9 July 2002; accepted in revised form 19 September 2002

Key words: electrocatalysis, methanol electrooxidation, nanoparticles, PtRu electrodes, Ru deposition

Abstract

Methanol oxidation electrocatalysts were prepared from Ru electrochemical or spontaneous deposition on commercial-grade carbon-supported Pt nanoparticles (Pt-Vulcan XC72, E-TEK). The resulting Ru coverage was estimated by cyclic voltammetry in supporting electrolyte. The maximum electrocatalytic activity for methanol oxidation at room temperature was observed at lower Ru coverage for spontaneous deposition than for electrodeposition; θ_{Ru} ~10% vs ~20%, respectively. On the other hand, higher current densities for methanol oxidation were obtained in the case of electrodeposited Ru. These two results were related to the presence of non-reducible ruthenium oxides in the spontaneous deposit. The present work provides evidence that (i) efficient DMFC electrocatalysts can be achieved by Ru deposition on Pt nanoparticles, and (ii) formation of a PtRu alloy is not a required condition for effective methanol electrooxidation.

1. Introduction

Methanol anodes with high electrocatalytic activity and low Pt loading are a key component for the development of an efficient and attractive electrochemical energy conversion technology based on the direct methanol fuel cell (DMFC) [1]. To date, the most efficient methanol anodes are based on platinum and ruthenium (for reviews, see [2, 3]). Whereas on Pt, methanol oxidation is poisoned by formation and adsorption of CO intermediates (CO_{ads}) [2–4], addition of Ru to Pt greatly enhances the rate of methanol electrooxidation [5, 6] through a bifunctional mechanism [6–8]. Measurements at Pt–Ru alloy electrodes of well-characterized surface composition showed that the activity for methanol electrooxidation at room temperature is maximum at low Ru coverage (<20% surface atoms) [9, 10]. On the other hand, several papers have provided evidence that formation of PtRu alloy is not a required condition for efficient electrocatalysis [6, 11, 12].

Although kinetic studies at Pt Ru alloy electrodes [9, 10, 13] and Ru-modified Pt(*h k l*) surfaces [14–16] provided fundamental understanding of the methanol oxidation mechanism, it remains necessary to optimize the active surface area/metal loading ratio in technical fuel cell electrodes [12, 17]. Typical DMFC anodes consist of carbon-supported or unsupported PtRu nanoparticles in contact with a proton exchange membrane (e.g., Nafion®) [2] and electrocatalysis of methanol oxidation at Pt nanoparticles is different from that at smooth Pt electrodes [18]. In addition to a particle size effect [19–22], the preparation method of the nanoparticles [23], the catalyst pretreatment [24] and eventually the physical and chemical properties of the carbon support [20, 25], may affect the activity for methanol electrooxidation. Comparison of various PtRu electrocatalysts thus requires an accurate determination of the electroactive surface area, of the mean particle size, and an evaluation of the actual Ru coverage. Particle size analysis can be performed by TEM [26].

On the other hand, estimation of the ratio Ru/Pt surface atoms by surface-sensitive techniques, such as STM, LEIS or AES [9, 12, 15, 16], are difficult to carry out in the case of PtRu nanoparticles. X-ray methods provide qualitative and, to some extent, quantitative data, although the measurements usually determine the amount of Ru in the bulk not at the surface of the nanoparticles [2, 27, 28]. In addition, no electrochemical method is commonly accepted for evaluating the Ru coverage because electrosorption of hydrogen on Pt and oxygenated species on Ru occur in a narrow range of potential [6]. We can anticipate that measurements based on Ru redox currents in the double layer region will be less accurate than for Pt(*h k l*) surfaces [29] because of the influence of the carbon support. Using cyclic voltammetry (CV), coupled with electrochemical quartz-crystal microbalance (EQCM) measurements, the amount of electrodeposited Ru was correlated to

the shift (compared to pure Pt) of the surface-oxide reduction peak [30]. However, this method is destructive because potential cycling up to the 'oxide region' irreversibly alters the electrocatalytic properties of the PtRu surface.

Concerning the preparation of PtRu electrodes, literature data indicates that Ru spontaneous and electrochemical deposition on Pt(*h k l*) electrodes are suitable methods for adjusting Ru coverage on Pt [12, 14, 16, 31–33]. Ru-modified Pt(1 1 1) also exhibits the highest activity for methanol oxidation among the PtRu surfaces [16]. On the other hand, Ru spontaneous deposition on unsupported Pt nanoparticles [34] or Ru electrodeposition on Pt–C electrode [35] has yielded efficient methanol oxidation electrocatalysts. Among the reported routes for producing PtRu nanoparticles [2, 27, 28], deposition of Ru adlayers on Pt nanoparticles appears as one of the most suitable methods for adjusting the Ru coverage while controlling the size of the particles.

In this paper, we present a kinetic study of methanol electrooxidation at PtRu nanoparticles. The electrochemical measurements were performed at glassy carbon electrodes coated with a thin film of carbon-supported electrocatalyst dispersed in a proton exchange membrane (Nafion®). This procedure allowed a very effective utilization of the electrocatalytic surface area, and hence an accurate elucidation of electrode kinetics [36]. The electrocatalysts were prepared from Ru electrochemical or spontaneous deposition on commercial-grade carbon-supported Pt nanoparticles (Pt-Vulcan XC72, E-TEK). The resulting Ru coverage was estimated from cyclic voltammetry (CV) in supporting electrolyte. We were thus able to investigate the influence of Ru coverage on the kinetics of methanol electrooxidation independently of any particle size effect and/or preparation method.

2. Experimental details

Solutions were prepared from concentrated $HClO_4$ (Suprapur, Merck), $RuCl_3$ and $Ru(NO)(NO_3)_3$ (Alfa Aesar), high purity grade methanol (Merck) and ultrapure water (MilliQ, Millipore). The electrocatalyst was a 30 wt.% Pt–C (Vulcan XC72) from E-TEK. As confirmed by TEM analysis, the Pt particles are homogeneous in size ($d = \sim 3.4$ nm), and close to the maximum in term of mass activity (A g^{-1} of Pt) for methanol electrooxidation [22]. The working electrode was prepared by coating a glassy carbon disc (3 mm dia.) with a thin film of Pt–C powder (E-TEK) and recast Nafion® [37]. The electrochemical experiments were conducted in conventional glass cells. The counter electrode was a glassy carbon plate and the reference electrode a calomel electrode (SCE) connected to the working electrode compartment via a Luggin capillary. The open circuit potential of a Pt electrode in H_2-saturated 0.1 M $HClO_4$ was −0.305 V vs SCE, that is, 0 V vs RHE (reversible hydrogen electrode). In the following, the potentials are quoted on the RHE scale. CV (0.05 to 1.00 V vs RHE, 20 mV s^{-1}) was carried out in N_2-purged 0.1 M $HClO_4$ to remove any surface contamination coming from the Nafion® solution (5 wt.%, Aldrich) used for preparing the working electrodes. The real Pt surface area was then estimated by integration of the $I/E(t)$ response in the hydrogen electrosorption region (i.e., 0.05 to 0.4 V vs RHE) assuming a theoretical quantity of electricity of 210 μC cm^{-2} of Pt.

Ru electrodeposition at Pt–C electrodes was carried out in a rotating electrode configuration (1000 rpm) by electrolysis of N_2-purged 0.1 M $HClO_4$ with 10^{-5} M $Ru(NO)(NO_3)_3$, because this complex does not yield any Ru spontaneous deposition (see below) [16, 30, 38]. After a contact time of about 10 min at open circuit potential, the potential was stepped to 1.0 V for 0.1 s and then to 0.55 V for 2 to 30 s. The deposition charge Q_{Ru} was obtained by subtraction of Q_{dl} to Q_{tot}, where Q_{dl} and Q_{tot} were calculated by integration of current against time response in ruthenium-free and Ru(NO)$(NO_3)_3$-containing electrolyte, respectively. Spontaneous deposition of Ru was carried out at open circuit potential by immersion for periods ranging from 5 to 3600 s in N_2-purged 0.1 M $HClO_4$ with 5×10^{-3} M or 5×10^{-4} M $RuCl_3$ [16]. Ageing for 2–3 weeks is necessary to obtain a deposition solution in which hydrated Ru complexes are formed from $RuCl_3$ [31]. UV-spectra of our deposition solution revealed the presence of Ru^{VI} species ($\lambda = 470$ nm) [39]. It is also emphasized that Ru spontaneous deposition is barely observed with solutions containing anions that strongly adsorb on Pt, such as (bi)sulfate anions [12]. After Ru deposition, the working electrode was removed from the deposition solution, thoroughly rinsed with water, and then transferred to a similar cell containing only 0.1 M $HClO_4$ for CV characterization (0.05 to 0.65 V, 20 mV s^{-1}). The upper potential limit was set to 0.65 V vs RHE, avoiding any irreversible ruthenium oxidation [30], and minimizing the effect of the electrochemical treatment on the Ru deposit structure. In the case of electrodes modified by Ru spontaneous deposition, reproducible voltammograms were obtained after five consecutive cycles.

The kinetics of methanol oxidation between 0.05 and 0.65 V vs RHE was measured by slow scan (5 mV s^{-1}) CV in N_2-purged 0.1 M $HClO_4$ with 0.1 M MeOH. Stationary measurements were also performed using the following potential program: E_{ox} (0.1 s) → 0.7 V (1 s) → E_{ox} (1800 s), with $0.4 \leqslant E_{ox} \leqslant 0.65$ V vs RHE.

3. Results and discussion

3.1. *Ru deposition on carbon-supported Pt nanoparticles*

Electrolysis at low overpotential of a dilute Ru $Ru(NO)(NO_3)_3$ solution were the experimental conditions considered as the most suitable for adjusting the

Ru coverage on the Pt nanoparticles while avoiding Ru deposition on the carbon support. As a first approach, we thus carried out EQCM experiments at a quartz crystal-supported Pt electrode with the aim of quantifying the amount of electrodeposited Ru under such experimental conditions (for experimental details see [38]).

Figure 1 shows the variation of the current intensity (I) and the interfacial mass (Δm) as a function of the electrolysis time (t) for a potential step from the open circuit potential to 0.4 V vs RHE. As shown in Figure 1(b), the $\Delta m/t$ response in $Ru(NO)(NO_3)_3$ solution (solid line) is shifted upward compared to that recorded in ruthenium-free solution (dashed line), indicating an interfacial mass increase due to Ru electrodeposition at the quartz crystal-supported Pt electrode. As expected the amount of electrodeposited Ru increases with increase in electrolysis time. It is however to be noticed that the variation of Δm with t becomes almost negligible at $t > 40$ s, suggesting a significant drop of the electrolysis yield after this period. On the other hand, the I/t transient response in $Ru(NO)(NO_3)_3$ solution does not exhibit the shape expected for a 3D-nucleation process with diffusion control [40], and the quantity of electricity corresponding to the initial portion of the curve (i.e., the sharp peak) is significantly larger than that required for recharging the electrode double layer (Figure 1(a): solid and dashed line, respectively). These observations are strong indications that electrolysis at a low overpotential of a diluted $Ru(NO)(NO_3)_3$ solution yields a Ru adlayer whose growth is kinetically limited by the discharge of the Ru complex on the Pt surface. The assumption of a 2D-deposition process is further supported by a previous EQCM study [38], as well as by STM surface analysis indicating that Ru electrodeposition at Pt(1 1 1) electrodes leads to the formation of 2D islands of several nanometers in diameter [12, 15], until $\theta_{Ru} \leqslant 40\%$ [41]. In the present study, we were hence able to calculate the Ru coverage (θ_{Ru}) of the Pt electrode from the overall mass gain $\Delta(\Delta m)$ determined by EQCM (Figure 1(b), [38]):

$$\theta_{Ru} = \frac{\Delta(\Delta m)}{M_{Ru} \times (Q_H/F)} \quad (1)$$

where M_{Ru} is the molecular weight of Ru (101.1 g mol^{-1}), and Q_H the H-adsorption charge on the Ru-free Pt surface (i.e., Q_H/F is thus the number of mole of Pt surface atoms).

Based on these preliminary results, quartz crystal-supported Pt electrodes with different Ru coverages were obtained by electrolysis for suitable periods. The electrolysis was stopped when the desired amount of Ru was electrodeposited (Equation 1). Figure 2(a) shows CV of unmodified and Ru-modified Pt electrodes in N_2-purged 0.1 M $HClO_4$. Upon addition of Ru, the charge associated with hydrogen electrosorption decreases, whereas the charge associated with the double layer increases, which is consistent with previously reported CV studies [6]. Figure 2(b) further shows that addition of Ru yields a significant decrease in the height of the peak at 0.12 V, assigned to hydrogen electrosorption on Pt(110)-like sites. In the following, we thus decided to use this electrochemical parameter to estimate the coverage of Pt with Ru. The Ru coverage (θ_{Ru} in Equation 1) was plotted as a function of the peak height decrease (δ), calculated using data such as those shown in Figure 2(b). The resulting curve clearly indicates a linear dependence between θ_{Ru} and δ (Figure 3, solid line), consistent with the assumption of a 2D-deposition of Ru on the Pt surface (see above). As this calibration curve was obtained for rather rough Pt surfaces (roughness factor of ~10), it might provide a convenient tool for evaluating the Ru coverage on Pt nanoparticles.

Electrolysis of $Ru(NO)(NO_3)_3$ solution was performed at Pt–C electrodes using conditions very similar to those for the quartz crystal-supported Pt electrodes (Section 2). Figure 4(a) shows CV of unmodified and Ru-modified Pt–C electrodes in N_2-purged 0.1 M $HClO_4$. An increase of the charge corresponding to the double layer is not clearly observed for Ru coverage

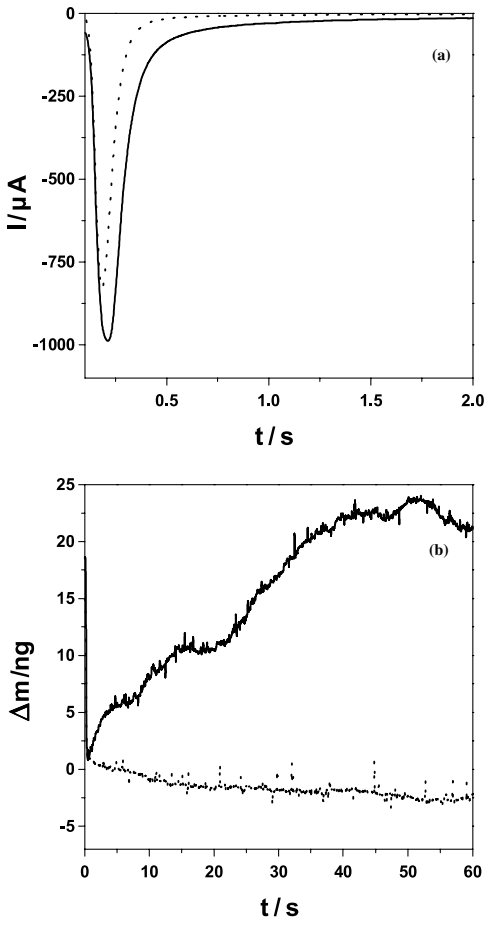

Fig. 1. (a) I/t transient response of a quartz crystal-supported Pt electrode in N_2-purged 0.1 M $HClO_4$ before and after addition of 2×10^{-4} M $Ru(NO)(NO_3)_3$ (dotted and solid lines, respectively). (b) Simultaneously recorded interfacial mass change (Δm). The potential was stepped from 1.0 V (0.1 s) to 0.4 V (60 s), after a contact time of about 10 min at open circuit potential. Geometric surface area 0.25 cm^2 and roughness factor ~10.

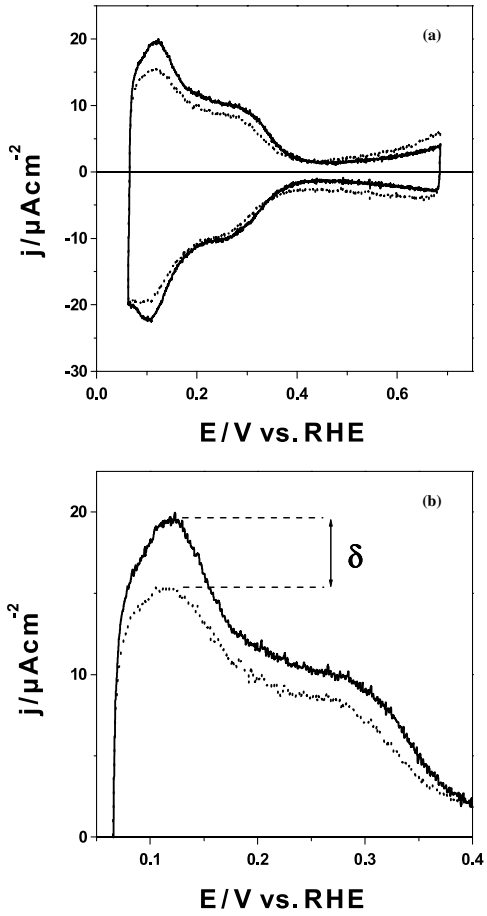

Fig. 2. (a) CV (20 mV s^{-1}) of a quartz crystal-supported Pt electrode in N_2-purged 0.1 M $HClO_4$ before and after Ru electrodeposition (solid and dotted lines, respectively). Ru coverage of about 11% was obtained by a potential step to from 1.0 V (0.1 s) to 0.4 V (240 s) in N_2-purged 0.1 M $HClO_4$ with 2×10^{-4} M $Ru(NO)(NO_3)_3$. (b) CV highlights in the potential range 0.05–0.4 V vs RHE.

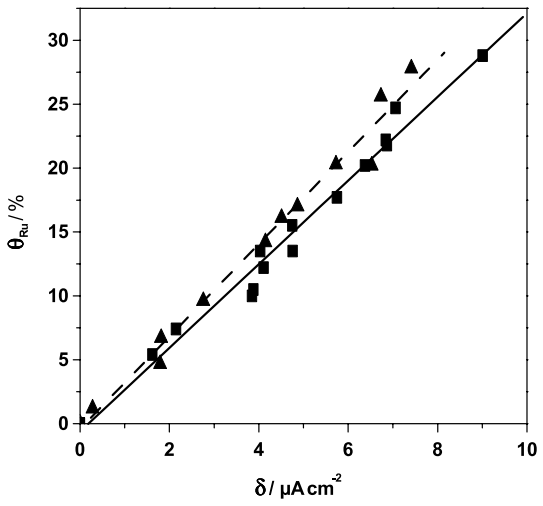

Fig. 3. Ru coverage (θ_{Ru}) as a function of parameter δ (see text) for quartz crystal-supported Pt (■) and Pt–C (▲) electrodes, respectively. Solid and dashed lines correspond to linear regressions. Ru was electrodeposited on the Pt–C electrodes by potential step from 1.0 V (0.1 s) to 0.4 V (2 to 30 s) in N_2-purged 0.1 M $HClO_4$ with 10^{-5} M $Ru(NO)(NO_3)_3$, after a contact time of about 10 min at open circuit potential.

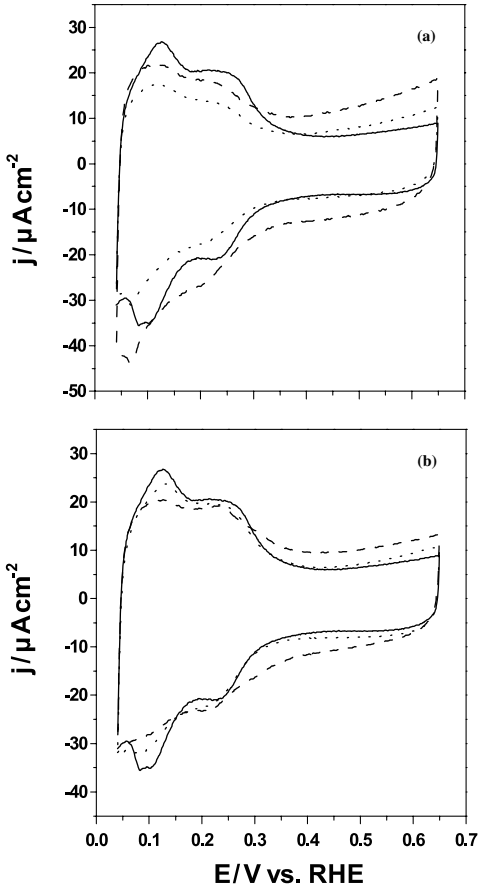

Fig. 4. Effect of the Ru coverage on CV (20 mV s^{-1}) of Ru modified Pt–C electrodes in N_2-purged 0.1 M $HClO_4$. (a) Ru electrochemical deposition: $\theta_{Ru} \approx 46\%$ (dashed line), 20% (dotted line) and 0% (solid line), respectively. (b) Ru spontaneous deposition: $\theta_{Ru} \approx 22\%$ (dashed line), 9% (dotted line) and 0% (solid line), respectively.

lower than 20% because of the effect of the carbon support in this potential region. As in the case of the quartz crystal-supported Pt electrode (Figure 2), CV in Figure 4(a) reveals a significant effect of Ru addition on the peak height at 0.12 V vs RHE. The observation of an effect of Ru addition on the H-electrosorption process also suggests that ruthenium is mainly electrodeposited on the Pt nanoparticles and not on the carbon support. Consequently, the coverage of the Pt nanoparticles with Ru can be calculated as follows:

$$\theta_{Ru}^{max} = \frac{Q_{Ru}/3F}{Q_H/F} \tag{2}$$

where Q_{Ru} is the deposition charge (see experimental) and Q_H/F the number of moles of Pt surface atoms. In Equation 2, it is also assumed that the reduction of the Ru ions to Ru metal involves three electrons and occurs with an electrolysis yield of 100%. As previously, the maximum Ru coverage (θ_{Ru}^{max} in Equation 2) was plotted against the peak height decrease (δ) at 0.12 V vs RHE, using data such as those shown in Figure 4(a). Figure 3 shows the resulting curve along with the data obtained from EQCM experiments (dashed and solid lines, respectively). Interestingly, $\theta_{Ru}^{EQCM} \sim \theta_{Ru}^{max}$ at low δ val-

ues, while the plot of θ_{Ru}^{EQCM} against δ is shifted downward with an increase in the parameter δ, and hence in the Ru coverage. In the present work, low values of Ru coverage correspond to very short electrolysis times (typically, $t \leqslant 5$ s). In such conditions, the electrolysis yield should be high, and hence $\theta_{Ru}^{EQCM} \sim \theta_{Ru}^{max}$. At higher values of Ru coverage corresponding to electrolysis times up to 30 s, we observe $\theta_{Ru}^{EQCM} < \theta_{Ru}^{max}$, likely because of a decrease in the electrolysis yield. Indeed it has been shown that the kinetics of Ru electrodeposition, relatively fast on Ru-free Pt surface, slows rapidly down as the Ru coverage increases [16] (see also Figure 1(b)). In the present work, the ruthenium concentration in the Nafion® phase is significantly larger than that in solution because of the Donnan effect thus increasing the electrodeposition rate at short electrolysis time. In conclusion, the θ_{Ru} against δ calibration curve derived from EQCM experiments takes into account the effect of the Ru coverage on the electrolysis yield (Figure 3). It might thus be a convenient tool for an evaluation of the Ru coverage of the Pt nanoparticles.

Ru spontaneous deposition was carried out by immersion of the Pt–C electrodes in 'aged' $RuCl_3$ solution. CV in N_2-purged 0.1 M $HClO_4$ of the resulting electrodes (Figure 4(b)) is comparable to that of the Ru-modified Pt–C electrodes prepared by Ru electrodeposition (Figure 4(a)). Noteworthy is the significant decrease compared to pure Pt of the peak height at 0.12 V (Figure 4(b)). We thus conclude that Ru-containing species were spontaneously deposited at the Pt nanoparticles | Nafion® interface. The Ru adlayers were stable in the investigated potential range (Figure 4(b)), consistent with the results reported for Pt(*h k l*) surfaces [16, 31]. Figure 5 shows the effect of the contact time and of the ruthenium solution concentration on the parameter δ. This varies slowly for contact times shorter than 10 s, because this is the period of time required for balancing the ruthenium concentrations within the recast Nafion® phase. An increase in ruthenium concentration in solution leads to an increase in the rate of spontaneous deposition because shorter contact times were required to obtain an equal value for the parameter δ. A limiting value, $\delta \approx 6\ \mu A\ cm^{-2}$, is, however, observed independently of the initial $RuCl_3$ concentration in solution. Using the data in Figure 5 along with the θ_{Ru} against δ plot from the EQCM experiments (solid line in Figure 3), we were able to estimate the amount of Ru spontaneously deposited on the Pt–C electrodes. As shown in Figure 5, the Ru coverage of the Pt nanoparticles reaches the limiting value of $\theta_{Ru} \approx 22\%$ (Table 1), consistent with the values reported in the case of unsupported Pt nanoparticles [34]. Similar values of Ru saturation coverage were also determined for Pt(1 1 1) from AES analysis and/or direct observations with STM [15, 16]. As the carbon-supported Pt nanoparticles used in the present study should exhibit large fractions of Pt(1 1 1) sites [42], this result provides confidence in the validity of our method for evaluating the Ru coverage of carbon-supported Pt nanoparticles. The observation of a saturation coverage, as on the θ_{Ru}/t response in Figure 5, might be related to the presence of non-reducible Ru oxides in the spontaneous deposit [43]. A possible explanation is that oxygen atoms might be shared between ruthenium and platinum, which deactivates the Pt sites for further Ru deposition. An 'electronic' effect of ruthenium oxides on the nearest Pt sites might also be considered.

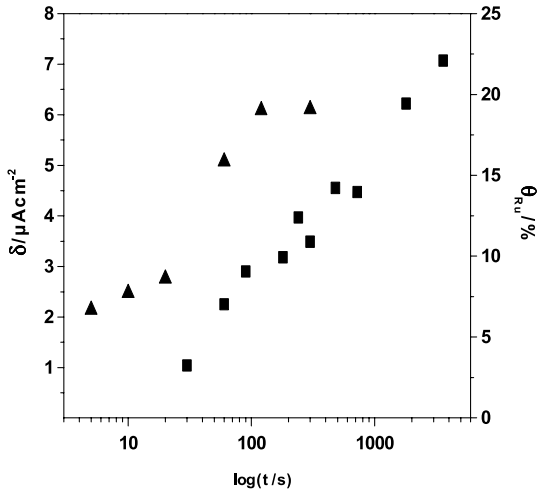

Fig. 5. Variation of the parameters δ and θ_{Ru} as a function of the contact time for Pt–C electrodes in 0.1 M $HClO_4$ with 5×10^{-3} M (▲) and 5×10^{-4} M (■) $RuCl_3$, respectively.

3.2. *Methanol electrooxidation at Ru-modified Pt nanoparticles*

Being able to prepare Pt–C electrodes with a controlled Ru surface composition, we investigated the effect of Ru coverage on the kinetics of methanol electrooxidation. This effect was explained by a bifunctional reaction mechanism [6]. In the potential region relevant for DMFC applications ($E < 0.5$ V), CO intermediates (CO_{ads}) are formed in a methanol dehydrogenation step at Pt sites (Equation 3). CO_{ads} is then oxidized to CO_2 (Equation 5) via adsorbed oxygenated species (OH_{ads}) formed by activation of water at Ru sites (Equation 4). The rate-determining step (r.d.s.) in this potential range

Table 1. Coverage of Pt(*h k l*) surfaces and Pt nanoparticles with Ru as estimated from (a) electrochemical measurements (b) or physicochemical analysis

Electrode	$[RuCl_3]$ /mol L^{-1}	Contact time /s	θ_{Ru} /%	Ref.
Pt(1 1 1)	5×10^{-5}	60	10 [a,b]	[31]
Pt(1 0 0)	5×10^{-5}	60	24 [a,b]	[31]
Pt(1 1 0)	5×10^{-5}	60	5 [a,b]	[31]
Pt–C	5×10^{-4}	60	7 [a]	present work
Pt black	1×10^{-3}	3600	20 [b]	[34]
Pt–C	5×10^{-4}	3600	22 [a]	present work

is likely the activation of water at the Ru sites (Equation 4) [44].

$$CH_3OH_{ads} \rightarrow CO_{ads} + 4H^+ + 4e^- \quad (3)$$

$$Ru + H_2O \rightarrow OH_{ads} + H^+ + e^-; E \geqslant 0.35\,V \text{ vs RHE} \quad (4)$$

$$CO_{ads} + OH_{ads} \rightarrow CO_2 + H^+ + e^- \quad (5)$$

In Equation 5, CO_{ads} stands for CO intermediates adsorbed either on Pt or Ru sites (or both), consistent with the reported effect of CO surface mobility on the overall reactivity [7, 12, 32, 45].

Figure 6 shows slow-scan CV in N_2-purged $HClO_4$ with 0.1 M CH_3OH of Ru-modified Pt–C electrodes prepared by either electrochemical (a) and (a′) or spontaneous (b) and (b′) deposition. As expected, addition of small amount of Ru shifts the onset of methanol oxidation to less positive potentials. However, increasing the coverage above 20–25% for electrodeposited Ru or 10–15% for spontaneously deposited Ru yields a further decrease in the methanol electrooxidation current. The volcano plots in Figure 7 confirm these observations. In the potential range 0.4 to 0.5 V vs RHE, the maximum in electrocatalytic activity towards methanol oxidation is observed for $\theta_{Ru} \sim 10\%$ in the case of spontaneous deposition and for $\theta_{Ru} \sim 20\%$ in the case of electrodeposition. This discrepancy might be related to the chemical nature of the Ru deposit. In this potential range, the Ru adlayers form reducible oxides [35] whereas the spontaneous deposit likely contains a fraction of Ru oxides that cannot be completely reduced (see UV-spectra in experimental and [43]). Consequently, sufficient amounts of oxygenated species to support reasonable CO_{ads} oxidation rates (Equation 5) could be formed at lower Ru coverage in the case of spontaneous deposits. On the other hand, a lower value of maximum current density was observed at Pt–C electrodes modified by Ru spontaneous deposition: 18 vs 34 A g^{-1} Pt (Figure 7). This result suggests that non-reducible Ru oxides deactivate the electrocatalytic surface for CO_{ads} oxidation. A similar result was observed in the case of Pt(*h k l*) surfaces, although not discussed [16]. The activity reported in Figure 7 are consistent with the assumption that metallic ruthenium (and/or reducible Ru oxides) is a required condition for effective methanol electrooxidation [1]. It is also conceivable that in the case of spontaneous deposit, the chemical nature of the Ru adlayer decrease the rate of CO_{ads} surface diffusion, and hence the oxidation kinetics [7, 12, 45]. Another possibility is a strong 'steric' or 'electronic' effect of Ru oxides on the Pt sites. This assumption is supported by the observation that most of the Pt surface atoms are

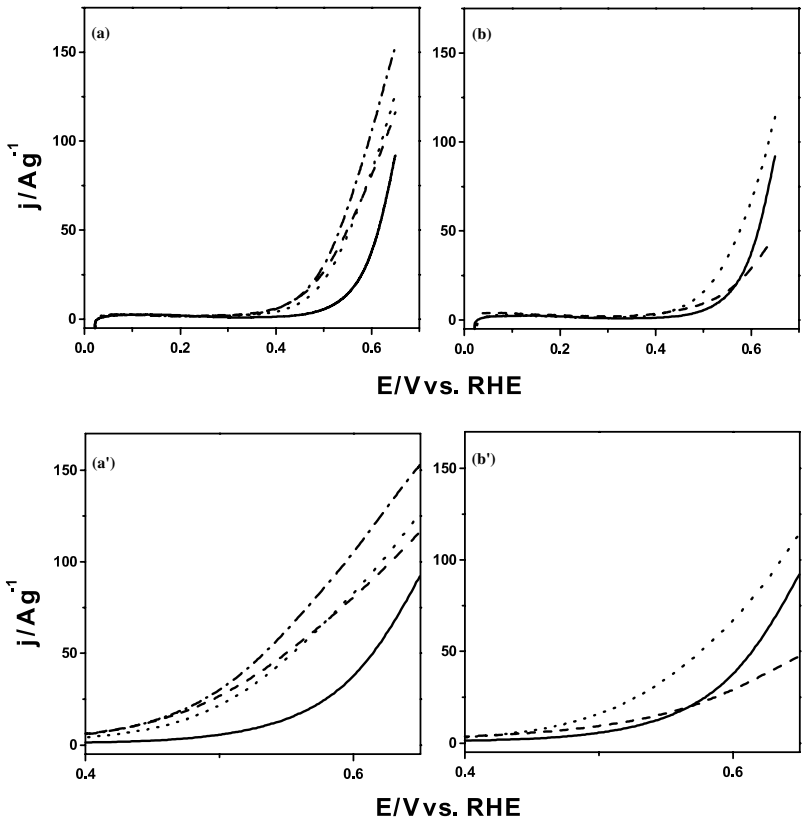

Fig. 6. (a) slow-scan (5 mV s^{-1}) CV of Ru-modified Pt–C electrode in N_2-purged 0.1 M $HClO_4$ with 0.1 M CH_3OH. (a) and (a′) Ru electrochemical deposition: $\theta_{Ru} \approx 33\%$ (dashed line), 20% (dash–dotted line), 10% (dotted line) and 0% (solid line), respectively. (b) and (b′) Ru spontaneous deposition: $\theta_{Ru} \approx 22\%$ (dashed line), 9% (dotted line), and 0% (solid line), respectively. (a′) and (b′): highlights in the potential range 0.4–0.65 V vs RHE of the voltammograms in (a) and (b), respectively.

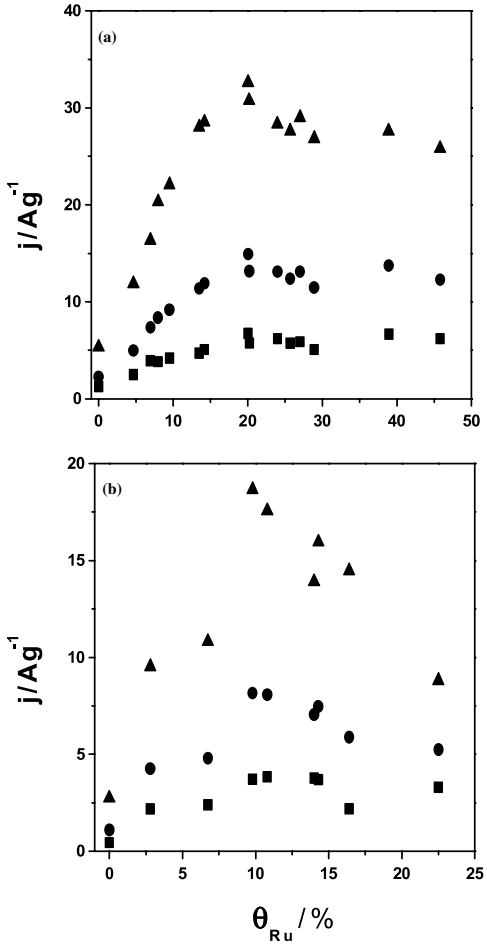

Fig. 7. Volcano plots for Ru-modified Pt–C electrodes prepared from (a) electrodeposition and (b) spontaneous deposition, respectively. Activities for methanol electrooxidation in N_2-purged 0.1 M $HClO_4$ with 0.1 M CH_3OH at 0.4 V (■), 0.45 V (●) and 0.5 V (▲), respectively, from slow-scan CV in Figure 6.

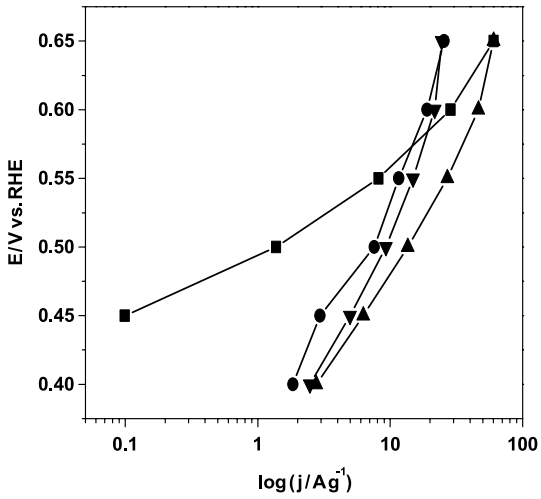

Fig. 8. Tafel plots at unmodified Pt–C electrode (■) and Ru-modified Pt–C electrodes (▲, ▼ and ●) in N_2-purged 0.1 M $HClO_4$ with 0.1 M CH_3OH. Ru electrochemical deposition: $\theta_{Ru} \approx 20\%$ (▲) and 46% (▼), respectively. Ru spontaneous deposition: $\theta_{Ru} \approx 10\%$ (●). Activities for methanol electrooxidation were determined after 30 min under stationary conditions.

Table 2. Activity of various PtRu catalysts for methanol electrooxidation at room temperature

Electrode	[CH_3OH] /mol L^{-1}	E_{ox} /V	Activity /A g^{-1}	Ref.
PtRu black (alloy)	0.5	0.4	1.9 [a]	[34]
Ru-modified Pt black	0.5	0.4	1.5 [a]	[34]
Ru-modified Pt–C	0.5	0.4	8.5 [b]	present work
Ru-modified Pt–C	0.1	0.4	2.8 [b]	present work
PtRu–C (non-alloy)	1.5	0.64	57 [b]	[12]
Ru-modified Pt–C	0.1	0.65	60 [b]	present work

Current intensity was measured under potentiostatic conditions after (a) 20 h or (b) 30 min.

not acting as nucleation sites in the case of Ru spontaneous deposition (Figure 5). Consequently, the presence of non-reducible Ru oxides may block the adsorption of methanol at the neighboring Pt sites.

Figure 8 shows the activities for methanol oxidation after 30 min at constant potential. At $E < 0.5$ V vs RHE, addition of Ru yields an increase of several order of magnitudes in activity. At $E > 0.55$ V vs RHE, the unmodified Pt–C electrode exhibits a greater activity than the Ru-modified Pt–C electrodes, which is consistent with previously reported results [10, 27]. This potential region is however not relevant for DMFC applications. There is also a much lower apparent Tafel slope for the Ru-modified Pt–C electrodes compared to the unmodified Pt–C electrode, suggesting different rate-determining steps for methanol electrooxidation [27, 36]. The data shown in Figure 8 further confirm a decrease in activity when the Ru coverage exceeds 20% for the electrodes prepared from Ru electrodeposition (in agreement with the volcano plot in Figure 7). The lower activity of the Ru-modified Pt–C electrode prepared from spontaneous deposition was also clearly observed under stationary conditions.

As shown in Table 2, the activity for methanol electrooxidation at room temperature of our Ru-modified Pt nanoparticles compares well with that of other PtRu electrocatalysts [12, 34]. This leads to the conclusion that efficient methanol electrooxidation catalysts can be prepared from Ru deposition, and especially electrodeposition, on Pt–C electrocatalyst.

4. Conclusion

This work shows that ruthenium can be effectively electrodeposited or spontaneously deposited on carbon-supported Pt nanoparticles dispersed in proton exchange membrane, such as Nafion®. Our results compare well with those previously reported for Pt(*h k l*) surfaces, which provides confidence in the validity of the chosen electrochemical method for evaluating the Ru coverage of carbon-supported Pt

nanoparticles. Saturation coverages of ca. 22% and 46% were observed in the case of spontaneous deposition and electrochemical deposition, respectively. This result was tentatively explained by the presence of non-reducible Ru oxides in the Ru adlayer formed by spontaneous deposition. The maximum in electrocatalytic activity towards methanol oxidation was observed at θRu $\sim$ 10% for spontaneous deposition and θRu $\sim$ 20% for electrodeposition. On the other hand, higher current densities for methanol oxidation were obtained in the case of electrodeposited Ru. We thus postulate that Ru adlayers with different chemical composition are formed depending on the deposition process. The spontaneous deposit may contain some non-reducible Ru oxides, consistent with the assumption that the activity of metallic ruthenium (and/or reducible Ru oxides) is greater than that of nonreducible Ru oxides. Finally, comparison of our data with previous work leads to the conclusion that efficient DMFC electrocatalysts can be achieved by Ru deposition on carbon-supported Pt nanoparticles. It also confirms that formation of a PtRu alloy is not a required condition for effective methanol electroxidation.

References

1. C. Lamy, J-M. Léger and S. Srinivasan, *in* J.O.M. Bockris, B.E. Conway and R.W. White (Eds), 'Modern Aspects of Electrochemistry', Vol. 34 (Kluwer Academic/Plenum, New York, 2001), pp. 53–115.
2. S. Wasmus and A. Kuver, *J. Electroanal. Chem.* **461** (1999) 14.
3. J-M. Léger, *J. Appl. Electrochem.* **31** (2001) 767.
4. R. Parsons and T. VanderNoot, *J. Electroanal. Chem.* **257** (1988) 9.
5. O.A. Petry, B.I. Podlovchenko, A.N. Frumkin and H. Lal, *J. Electroanal. Chem.* **10** (1965) 253.
6. M. Watanabe and S. Motoo, *J. Electroanal. Chem.* **60** (1975) 267.
7. J. Munk, P.A. Christensen, A. Hamnett and E. Skou, *J. Electroanal. Chem.* **401** (1996) 215.
8. H. Wang, C. Wingender, H. Baltruschat, M. Lopez and M.T. Reetz, *J. Electroanal. Chem.* **509** (2001) 163.
9. H.A. Gasteiger, N. Markovic, P.N.J. Ross and E.J. Cairns, *J. Electrochem. Soc.* **141** (1994) 1795.
10. A. Kabbabi, R. Faure, R. Durand, B. Beden, F. Hahn, J-M. Léger and C. Lamy, *J. Electroanal. Chem.* **444** (1998) 41.
11. M. Watanabe and S. Motoo, *J. Electroanal. Chem.* **60** (1975) 275.
12. K.A. Friedrich, K.P. Geyzers, A.J. Dickinson and U. Stimming, *J. Electroanal. Chem.* **524–525** (2002) 261.
13. R. Ianniello, V.M. Schmidt, U. Stimming, S.J. and A. Wallau, *Electrochim. Acta* **39** (1994) 1863.
14. E. Herrero, K. Franaszczuk and A. Wieckowski, *J. Electroanal. Chem.* **361** (1993) 269.
15. E. Herrero, J.M. Feliu and A. Wieckowski, *Langmuir* **15** (1999) 4944.
16. G. Tremiliosi-Filho, H. Kim, W. Chrzanowski, A. Wieckowski, B. Grzybowska and P. Kulesza, *J. Electroanal. Chem.* **467** (1999) 143.
17. L. Liu, R. Viswanathan, Q. Fan, R. Liu and E.S. Smotkin, *Electrochim. Acta* **42** (1998) 3657.
18. P.A. Christensen, A. Hamnett, J. Munk and G.L. Troughton, *J. Electroanal. Chem.* **370** (1994) 251.
19. A. Kabbabi, F. Gloaguen, F. Andolfatto and R. Durand, *J. Electroanal. Chem.* **373** (1994) 251.
20. T. Frelink, W. Visscher and J.A.R. van Veen, *J. Electroanal. Chem.* **382** (1995) 65.
21. Y. Takasu, T. Iwasaki, W. Sugimoto and Y. Murakami, *Electrochem. Comm.* **2** (2000) 671.
22. S.L. Gojkovic and T.R. Vidakovic, *Electrochim. Acta* **47** (2001) 633.
23. A. Kelaidopolou, E. Abelidou and G. Kokkinidis, *J. Appl. Electrochem.* **29** (1999) 1255.
24. B.D. McNicol and R.T. Short, *J. Electroanal. Chem.* **81** (1977) 249.
25. F. Gloaguen, J-M. Léger and C. Lamy, *J. Appl. Electrochem.* **27** (1997) 1052.
26. V. Radmilovic, H.A. Gasteiger and P.N.J. Ross, *J. Catal.* **154** (1995) 98.
27. T.J. Schmidt, H.A. Gasteiger and R.J. Behm, *Electrochem. Comm.* **1** (1999) 1.
28. Z. Jusys, T.J. Schmidt, L. Dubau, K. Lasch, L. Jorissen, J. Garche and R.J. Behm, *J. Power Sources* **105** (2002) 297.
29. W. Chrzanowski, H. Kim and A. Wieckowski, *Catal. Lett.* **50** (1998).
30. T. Freelink, W. Visscher and J.A.R. van Veen, *Langmuir* **12** (1996) 3702.
31. W. Chrzanowski and A. Wieckowski, *Langmuir* **13** (1997) 5974.
32. H. Massong, H. Wang, G. Samjeske and H. Baltruschat, *Electrochim. Acta* **46** (2000) 701.
33. J.C. Davies, B.E. Hayden, J.D. Pegg and M.E. Rendall, *Surf. Sci.* **496** (2002) 110.
34. P. Waszczuk, J. Solla-Gullón, H-S. Kim, Y.Y. Tong, V. Montiel, A. Aldaz and A. Wieckowski, *J. Catal.* **203** (2001) 1.
35. U. Koponen, T. Peltonen, M. Bergelin, T. Mennola, M. Valkiainen, J. Kaskimies and M. Wasberg, *J. Power Sources* **86** (2000) 261.
36. F. Gloaguen, T. Napporn, S. Donon, M-J. Croissant, S. Berthelot, J-M. Léger, C. Lamy and S. Srinivasan, *in* J. McBreen (Ed.), 'Electrode Materials and Processes for Energy Conversion and Storage IV', Vol. 97-13, The Electrochemical Society, Pennington (1998), pp. 131–138.
37. F. Gloaguen, F. Andolfatto, R. Durand and P. Ozil, *J. Appl. Electrochem.* **24** (1994) 863.
38. F. Vigier, F. Gloaguen, J-M. Léger and C. Lamy, *Electrochim. Acta* **46** (2001) 4331.
39. R.C. Walker, M. Bailes and L.M. Peter, *Electrochim. Acta* **44** (1998) 1289.
40. B. Scharifker and G. Hills, *Electrochim. Acta* **28** (1983) 879.
41. W.F. Lin, M.S. Zei, M. Eiswirth, G. Ertl, T. Iwasita and W. Vielstich, *J. Phys. Chem. B* **103** (1999) 6968.
42. K. Kinoshita, *J. Electrochem. Soc.* **137** (1990) 845.
43. H. Kim, I. Rabelo de Moraes, G. Tremiliosi-Filho, R. Haasch and A. Wieckowski, *Surf. Sci.* **474** (2001) L203.
44. D. Aberdam, R. Durand, R. Faure, F. Gloaguen, J-L. Hazemann, E. Herrero, A. Kabbabi and O. Ulrich, *J. Electroanal. Chem.* **398** (1995) 43.
45. K.A. Friedrich, K.P. Geyzers, F. Henglein, A. Marmann, U. Stimming and R. Vogel, *Z. Phys. Chem.* **208** (1999) 137.